Contents lists available at ScienceDirect

Science of the Total Environment

journal homepage: www.elsevier.com/locate/scitotenv



Potential fate of wetland soil carbon in a deltaic coastal wetland subjected to high relative sea level rise

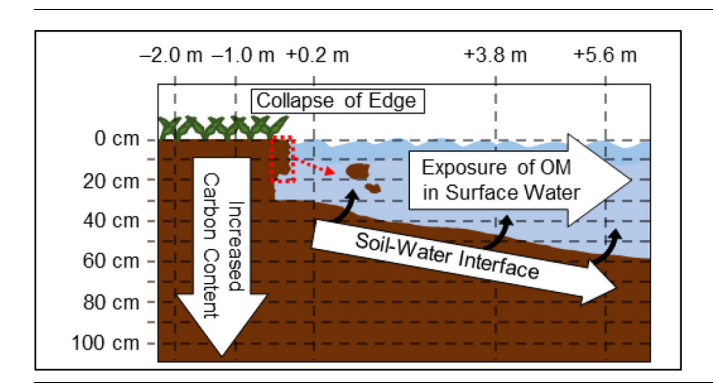


Benjamin J. Haywood a, Michael P. Hayes a, John R. White b,*, Robert L. Cook a,*

HIGHLIGHTS

- Collapse and degradation of coastal wetland marsh carbon.
- Degradation of submerged marsh
- · Release of stored carbon into bay water.

G R A P H I C A L A B S T R A C T



ARTICLE INFO

Article history: Received 18 August 2019 Received in revised form 21 October 2019 Accepted 23 October 2019 Available online 21 November 2019

Kevwords: Coastal wetland erosion Degradation of coastal wetland organic matter CO2 increase Ultraviolet-Visible (UV-Vis) Fluorescence excitation-emission matrices (EEMs)

ABSTRACT

The fate of soil carbon in eroding coastal wetlands is of great concern, given the potential for a feedback loop from coastal wetland soil that would dramatically increase atmospheric CO₂ concentrations. The biogeochemical transformations and overall fate of this soil carbon upon coastal erosion were investigated through geophysical and spectroscopic analysis of soil and associated dissolved organic matter. Bay water and core sections were collected across transects encompassing both intact and eroded, submerged, sections of a coastal marsh in Barataria Bay, Louisiana. We noted: i) a vertical increase in carbon content, humification of organic matter, and decrease in biotic degradation with depth at all sites; ii) an erosion and ultimate collapse of the top \sim 0–20 cm of the intact marsh's edge into the bay water due to the undercutting caused by tidal/wave forces; iii) the loss of the stored carbon from the submerged site's top 10 cm layer; and iv) leaching, dilution, abiotic, and biotic degradation of the marsh carbon due to the exposure to the bay water. This erosion and degradation of wetland soil carbon stores demonstrates the potential impact of rising sea levels on the future fate of coastal wetland carbon and atmospheric CO2

© 2019 Elsevier B.V. All rights reserved.

1. Introduction

Wetlands account for 5-6% of the world's land surface vet hold approximately one-third of the world's soil carbon (Choi and Wang, 2004). Coastal wetlands (i.e., saltwater marshes and mangroves) sequester an order of magnitude more carbon than an equivalent area of terrestrial forests or peatlands (Chmura et al., 2003; Mcleod et al., 2011). The high rates of primary production and persistent anaerobic condition of coastal wetland soils allow for significant carbon sequestration rates averaging of 210 g CO₂ m² y⁻¹ (Mcleod et al., 2011). Louisiana coastal wetlands were

^a Department of Chemistry, Louisiana State University, Baton Rouge, United States

b Department of Oceanography & Coastal Sciences, Louisiana State University, Baton Rouge, United States

^{*} Corresponding authors. E-mail addresses: jrwhite@lsu.edu (J.R. White), rlcook@lsu.edu (R.L. Cook).

formed from the vertical accumulation of both autochthonous-derived organic matter (OM) and allochthonous river-derived mineral sediment (DeLaune et al., 1994). The OM in these wetlands can be divided into: i) easily degraded low molecular weight (MW) labile OM (e.g., carbohydrates and fatty acids) and ii) slowly degraded high MW refractory OM (e.g., tannins and lignin) (Reddy and DeLaune, 2008). Labile OM is utilized by microbes within the soil profile and is ultimately recycled back into the system. Refractory OM is not easily utilized by microbes and must first undergo photo- and/or extracellular enzymatic degradation to become labile OM (Fichot and Benner, 2012; Reddy and DeLaune, 2008).

Recent studies suggest that sea level rise rate acceleration poses a threat to coastal wetland ecosystems and their sequestered carbon (i.e., OM) (Pfeffer et al., 2008; Vermeer and Rahmstorf, 2009). Globally, it is estimated that coastal wetland coverage will be reduced by 46–59% by the end of this century, based on current sea level rise predictions alone (Spencer et al., 2016). In Louisiana, the combined effects of regional coastal subsidence is estimated at 5–16 mm y $^{-1}$ and eustatic sea level rise adds an additional 3.4 mm y $^{-1}$, resulting in coastal Louisiana experiencing higher rates of relative sea level rise compared to most of the world's coastlines (Kolker et al., 2011). This condition allows a unique opportunity to investigate the effects of predicted "future" rates of sea level rise on coastal Louisiana marshes today, before occurring in coastal marshes along more stable coastlines in the near future (Sapkota and White, 2019).

The increased sea level rise in Louisiana, along with other contributing factors, results in erosion (e.g., collapse and submergence) of the wetland edge, leading to a stepwise conversion of vegetated marsh into open water (Li et al., 2011; Steinmuller et al., 2019). Currently, this process has resulted in ~ 25.9 km² of wetland loss in the Barataria Bay, Louisiana, annually (Penland et al., 2000). After erosion occurs, the collapsed OM can be either reburied and stored within the bay sediment or mineralized and released as CO₂ into the atmosphere (Steinmuller et al., 2019). The submergence of the wetland soil allows oxygen-rich (aerobic) bay water to penetrate the top layers (~10-30 mm) where an aerobic-anaerobic interface is created (Reddy and DeLaune, 2008). This interface could allow for the leaching of the submerged OM into the bay water as well as dilution of the OM within the pore water of the submerged wetland soil. Exposure to the bay water and oxygen could result in increased photo- and/or extracellular enzymatic degradation of the OM, with conversion to labile DOM. The labile OM could then be degraded by microbial activity (Haywood et al., 2018), leading to the release of the previously sequestered/stored carbon. Thus, the fate of the previously sequestered carbon, and its fate upon tidal/wave erosion is critical to the understanding of the magnitude of the amount of carbon being released from the eroding coastal wetlands in LA as well as predicting the fate of wetland-dominated coastlines in the future and consequent impacts on atmospheric greenhouse gases budgets going forward (FitzGerald et al., 2008; Matear, 2004).

Geophysical properties, such as: bulk density (BD), loss on ignition (LOI), and TC measurements have long-standing use in carbon content assessments of wetland soils (Hoogsteen et al., 2015; Perie and Ouimet, 2008; Van de Broek et al., 2016; Watanabe et al., 2005). Although useful, such measurements do not provide a detailed understanding of OM biogeochemical transformations. Unlike the pore water dissolved organic matter (DOM), which is measured in parts per million (ppm), the soil OM (SOM) carbon is measured in parts per hundred (pph) and does not show noticeable fluctuations for recent (short-term) degradation processes. Since the majority of short-term degradation processes take place in the aqueous phase, spectroscopic indicators can be used to identify changes in pore water DOM with depth (Clark et al.,

2014; Wang et al. 2013). To identify the biogeochemical transformations, the qualitative and quantitative properties of the dissolved organic matter (DOM) can be analyzed using a combination of dissolved organic carbon, ultraviolet-visible (UV-Vis), fluorescence excitation-emission matrix (EEM), and parallel factor (PARAFAC) analysis (Cook et al., 2009; Haywood et al., 2018; Kolic et al., 2014). These measurements have been previously applied to determine the biogeochemical transformations and fate of OM in both estuarine surface water (Bianchi et al., 2011; Haywood et al., 2018; Kolic et al., 2014) and pore water of wetland soil (Chow et al., 2012; Clark et al., 2014; Wang et al., 2013).

The goal of this study was to identify the impact of tidal/wave-induced edge erosion on coastal wetland-stored OM from both a physical and chemical perspective. This goal has been achieved by using a combination of the geophysical and spectroscopic techniques to examine the OM stored up to 100 cm from the surface of the marsh at the interface of the eroding edge and by determining the biogeochemical transformations and fate of the OM. This is, to our knowledge, the first time that such a detailed analysis of wetland soil OM was analyzed at such a vital interface. This multifaceted approach can provide an improved understanding of the carbon biogeochemical transformation, and fate of the OM and associated carbon in a coastal marsh subjected to high relative sea level rise, a condition to be realized globally within the next 1/2 century.

2. Materials and methods

2.1. Study area

The study area (GPS coordinates: 29.443583, -89.899722) is located on the northeast edge of Barataria Bay, within the Barataria Basin, Louisiana (Fig. 1). The *Spartina alterniflora*-dominated marsh faces the open bay and therefore experiences > 1 m of edge erosion annually (Levine et al., 2017; Sapkota and White, 2019). Three

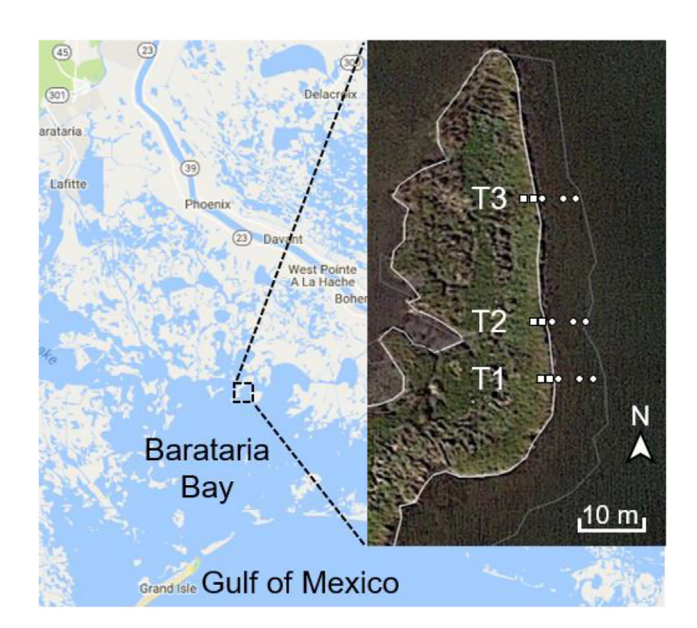


Fig. 1. Google earth satellite images of the Barataria Bay, Louisiana with (inset) section of the study site with sampling transects. An outline of the study site marsh perimeter as of November 2016 (white line) (most recent satellite image available) and October 2011 (grey line) has been provided to delineate marsh edge erosion over time. The cores are arranged West to East across each transect identified as intact marsh (-2.0 m and -1.0 m (\square)) and submerged marsh (+0.2 m, +3.8 m, and +5.6 m (\bigcirc)).

shore-normal transects were established spanning the intact marsh, 2 m inland, to 5.6 m off the marsh edge into the open bay (Fig. 1). Transects were sampled on March 10 and November 10, 2017 to investigate any seasonal effects. Air temperature, water temperature, salinity, and dissolved oxygen data were collected from the United States Geological Survey (USGS) station in Barataria Bay North of Grand Isle, Louisiana (USGS station 07380251) (USGS, 2017) for the sampling dates (Table S1.1). Water depth profiles of the submerged marsh along each transect were collected with a metered pole. A comprehensive bathymetric profile of the estuarine bottom from 7 to 120 m was collected (Figure S1.1) using a Garmin Echomap 50 and the description of method used for the depth profile determination are provided in Supporting Information S1.

2.2. Water sample collection

Surface water samples were collected off the edge of the marsh at each transect 10 cm below the water surface (the bay water has been found to be well mixed and homogeneous, as samples collected at top, middle, and bottom depths were found to be statistically (p > 0.05) similar, (Table S1.2 of Supporting Information S1 for further details). The sample collection, processing, and storage was performed following previously published procedure (Haywood et al., 2018).

2.3. Soil sample collection

Core samples were collected at five stations across each of the three transects, each consisting of two intact marsh stations and three eroded, submerged, sites. The intact marsh sites were located at 2.0 and 1.0 m inland from the marsh edge (termed intact sites – 2.0 m and –1.0 m) and the three submerged marsh sites were located at 0.2, 3.8, and 5.6 m off the marsh edge into the bay (termed submerged sites + 0.2, +3.8, and + 5.6 m) (Fig. 1). The cores were extruded in the field, sectioned into 10 cm increments, and sealed in polyethylene bags. The samples were stored on ice during transport and refrigerated at 4 °C until processing. The 10 cm core sections were weighed and centrifuged at 1792 G-force (i.e., 4000 rpm) for ten minutes to separate and collect the pore water. The pore water was removed, filtered, and stored identically to surface water samples until analysis.

2.4. Solid sample and carbon analysis

Bulk density (BD) was determined by drying a sub-sample of each core section, dried at 60 °C until constant weight, and back calculated to the whole soil segment. The dried sub-sample was then ground and combusted in a Thermo Scientific muffle furnace at 550 °C for 4 h to determine loss on ignition (LOI), a proxy for organic matter (Wright et al., 2008). Total carbon (TC) was determined on the dried and ground sub-sample of the March 10, 2017 sampling data using a Carlo-Erba NA1500 CNS Analyzer (Haak-Buchler Instruments, Saddlebrook, NJ). Filtered water samples (i.e., pore and bay surface) were analyzed for dissolved organic carbon (DOC) as described in previously published procedure (Haywood et al., 2018).

2.5. Spectroscopic analysis

The UV–Vis absorbance spectra and fluorescence EEMs were processed following a previously published procedure (Haywood et al., 2018), in which samples having absorbance above 0.900 A. U. (arbitrary units) were diluted by a factor of two with 18 Ωm Milli-Q deionized water (Kothawala et al., 2013). The UV–Vis absorbance spectra were collected between 200 and 600 nm utilizing a

Cary 100 Spectrophotometer, a 0.5 nm bandpass, and a 1 cm quartz cell. Fluorescence EEMs were collected on a Spex Fluorolog-3 spectrofluorometer utilizing a 1 cm quartz cell, with excitation wavelengths between 250 and 550 nm, and emission wavelengths between 250 and 600 nm, with 5 nm increments for both. Along with sample EEMs, blank EEMs of Milli-Q water were collected daily. To minimize temperature effects, samples for UV-Vis and fluorescence analysis were allowed to warm up to the room temperature and were shielded from light prior to analysis. Indicators from the UV-Vis spectra and fluorescence EEMs were determined following previously published procedures (Bianchi et al., 2011; Haywood et al., 2018; Kolic et al., 2014), with a full list of indicators determined as well as their description, chemical information, and ecological information being provided in Table 1.

The PARAFAC analysis of the sample EEMs (March 10 and November 10, 2017) was performed and the identities of components were determined following previously published procedure (Haywood et al., 2018), with further discussion of the method provided in Supporting Information S2. The components determined from the PARAFAC analysis as well as their description, chemical information, and ecological information are provided in Table 1.

2.6. Statistical analysis

The data from the two sample periods, collected on March 10 and November 10, 2017, were processed separately. The mean value and standard error of the mean for a given depth of a site or average of sites was determined by averaging the equivalent depth and site(s) from the replicate transects. Statistical analysis was performed using a two-tailed student's t-Test with twosamples assuming equal variances and α equal to 0.05. The correlation between the March 10 and November 10 data was determined through Pearson's product moment correlation of the transects mean value of each 10 cm section at each site (Table S3.1 of Supporting Information S3). Analysis of the geophysical and spectroscopic measurements vertical trends for each site was preformed using analysis of variance (ANOVA) ($\alpha = 0.05$) (Table S4.1 of Supporting Information S4). Additionally, a comparison of the horizontal similarities of the average intact sites 10 cm section to the submerged sites at an equivalent depth were performed using ANOVA ($\alpha = 0.05$) (Table S5.1 of Supporting Information S5).

3. Results and discussion

3.1. Study site conditions and sample alignment

The open bay adjacent to the marsh (including sites: +0.2, +3.8, and + 5.6 m) was previously an intact vegetated marsh, which has undergone 1.5 m of edge erosion per year since 2011 (Fig. 1) (Sapkota and White, 2019). At 20 m off the marsh edge, the estuarine bottom reaches a steady depth profile of 1.384 ± 0.089 (n = 4) m (Figure S1.1), indicating consistent depth due to wave energy within the open waters of the bay (Reddy and DeLaune, 2008). The depths of the submerged sites cores 10 cm sections were hung to the intact sites cores at a consistent datum using the average of the replicate submerged sites transects depth profiles, with the top of the marsh set as 0 cm (Fig. 2). For example, the top 0-10 cm layer of the submerged site + 3.8 m is equivalent to the depth of 50-60 cm from the surface of the intact marsh as the original 50 cm of soil is now lost (Fig. 2). This horizontal alignment of the sites was used throughout the following discussion to describe the location of each sample. At the study site, tidal/wave forces undercut the top $\sim 0-20$ cm of the marsh's edge, resulting in this bulk section collapsing and falling into the bay below (Fig. 2).

 Table 1

 Full list of indicators determined including: description, chemical information, and ecological information, for both spectroscopy and PARAFACs variables.

Measurement	Description	Chemical information	Ecological information	Reference					
UV-Vis indicators									
Spectral slope (S ₂₇₅)	Linear fit of the Napierian absorption coefficient spectrum from 275 to 295 nm	Lignin's molecular weight (MW), high values indicate low MW and low values indicating high MW	Photodegradation transformation lignin from high MW to low MW and degrades DOM	Fichot and Benner, 2012; Weishaar et al., 2003					
Fluorescence ir	Fluorescence indicators								
Fluorescence index (FI)	I_{em} at 450 nm (biological) divided by I_{em} at 500 nm (terrestrial) with Ex. 370 nm	DOM parent composition (terrestrial vs. aquatic)	The source of the DOM is indicated by values (1.9- aquatic) and (1.4-1.5-terrestrial)	McKnight et al., 2001					
Biological index (BIX)	l_{em} at 380 nm (protein) divided by l_{em} at 430 nm (biological) with Ex. 310 nm $$	Freshness of protein pool as DOM is degraded	Recent biological activity production of protein associated with the DOM pool	Huguet et al., 2009					
Humification index (HIX)	Sum of I_{em} 435–480 nm divided by sum I_{em} 300–345 nm pulse sum of I_{em} 435–480 nm with Ex. 254 nm	Red Shifting of fluorophores, the degree of humification	Decomposition of DOM contributing to bioavailability and the degree of humification	Ohno, 2002					
PARAFAC component indicators									
Fluorophore A	Peak signals Ex./Em. (nm): 270 (3 0 5)/410, historically peaks A and M	Lower degree of conjugation and abundance of functional groups; aromatic, carboxyl, and hydroxyl	Aqueous sourced, recently produced material with low MW and degree of and humification	Parlanti et al., 2000					
Fluorophore B	Peak signals Ex./Em. (nm): 275/325, historically peak T	Biological sourced DOM represented as dissolved amino acids in system	Identified as Tryptophan-like, result of biological activity (i.e., exudation spillage of cell)	Parlanti et al., 2000; Weishaar et al., 2003					

^{*}A similar table can be seen in Haywood, B. J.; White, J. R.; Cook, R. L., Investigation of an early season river flood pulse: Carbon cycling in a subtropical estuary. Science of The Total Environment 2018, 635, 867–877.

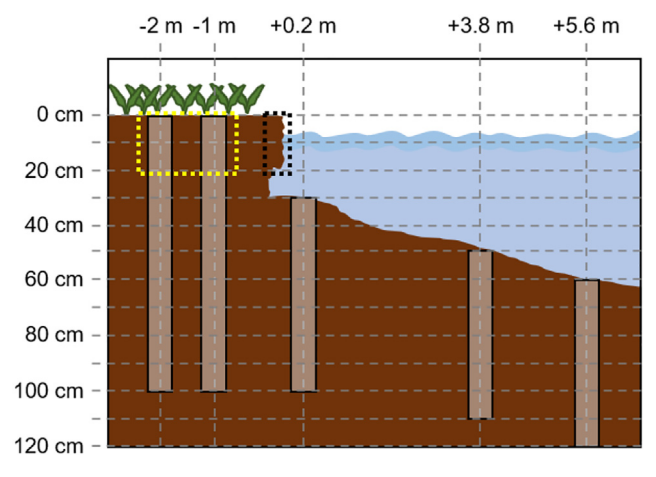


Fig. 2. Graphical representation of the horizontal alignment of the submerged sites 10 cm core sections to the intact site's core sections using the marsh surface as a consistent datum. Black dashed box represents the collapsing marsh's ~ 0–20 cm edge and yellow dashed box represents its corresponding "intact marsh model". The bottom profile of the submerged sites is based on a bathymetric profile (Figure S1.1). (For interpretation of the references to colour in this figure legend, the reader is referred to the web version of this article.)

The 0–10 and 10–20 cm sections of sites –2.0 m and –1.0 m of the three transects were combined to give a representative "intact marsh model" of the not yet eroded marsh edge soil (Fig. 2).

During the sample collection periods, the bay had nearly identical (within one standard error) values for water temperature, salinity, dissolved oxygen, and water height (Table S1.1) and the 10 cm mean spectroscopic indicator values at each site between the two sampling dates correlated positively (r = 0.24 to 0.99) (n = 55), with most having a very strong positive correlation with increasing depth from the surface of the marsh (Table S3.1). The strong positive relationship between the indicators of the two sample collection periods reveals that there is no seasonal impact on the OM in the intact and submerged marsh soil. Instrument failure resulted in the loss of the March 10, 2017 DOC data. Given the strong positive correlations between the sample collection periods and the lack of the March 10, 2017 DOC data, the November 10, 2017 data are used for the discussion below. The matching trends

for the available March 10, 2017 data are presented in the Supporting Information S3.

For the purposes of the discussion to follow, we will differentiate between abiotic and biotic degradation affecting carbon, where abiotic degradation is defined as occurring outside the microbial cell and refers to photo- and extracellular enzymatic cellular degradation and biotic degradation is defined as occurring inside the cell and refers to OM consumption and then later production of aquatic and protein-like OM (i.e., microbial activity).

3.2. Vertical changes in geophysical and biogeochemical properties

An increase of the SOM concentration with depth was indicated for all sites by a matching increasing trend of LOI value with depth (Table S4.1 and Fig. 3). This observation is supported by the trend of increasing TC concentration and decreasing BD values (lower mineral content) with depth (Table S4.1 and Fig. 3). Overall, these trends are indicative of increased carbon concentration with depth for all sites along the transect. This increase in carbon concentration with depth identified here is likely the result of changes in Barataria Bay, LA, once a fresh marsh prior to its current salt marsh conditions, such that the deposition environment has changed (Parlanti et al., 2000; Sapkota and White, 2019; Steinmuller et al., 2019).

For all sites there is a transition (indicative of humification) from labile OM in the top of the cores to refractory OM in lower sections, as indicated by the increase of spectroscopically determined indicators of MW of lignin-like components (inverse S₂₇₅ value) (Fichot and Benner, 2012) and degree of humification (HIX) (Ohno, 2002) (Table S4.1 and Fig. 3). Further support of the build-up and humifaction of the OM with depth is indicated by the increase in terrestrial nature (inverse FI value) (McKnight et al., 2001) and aquatic-like sourced OM (Fluorophore A) (Parlanti et al., 2000) with depth (Table S4.1 and Fig. 3). A decrease in biotic degradation with depth for all sites was identified by the decreasing trend of spectroscopically determined indicators of protein-like OM (Fluorophore B) (Parlanti et al., 2000) and "freshness" of OM (BIX) (Huguet et al., 2009) (Table S4.1 and Fig. 3).

Overall, all sites along the transect exhibit the same vertical trend of increased OM content, humification, and decreased biotic degradation from the surface of the cores to deeper layers. The changing values of the spectroscopic indicators, from the top of

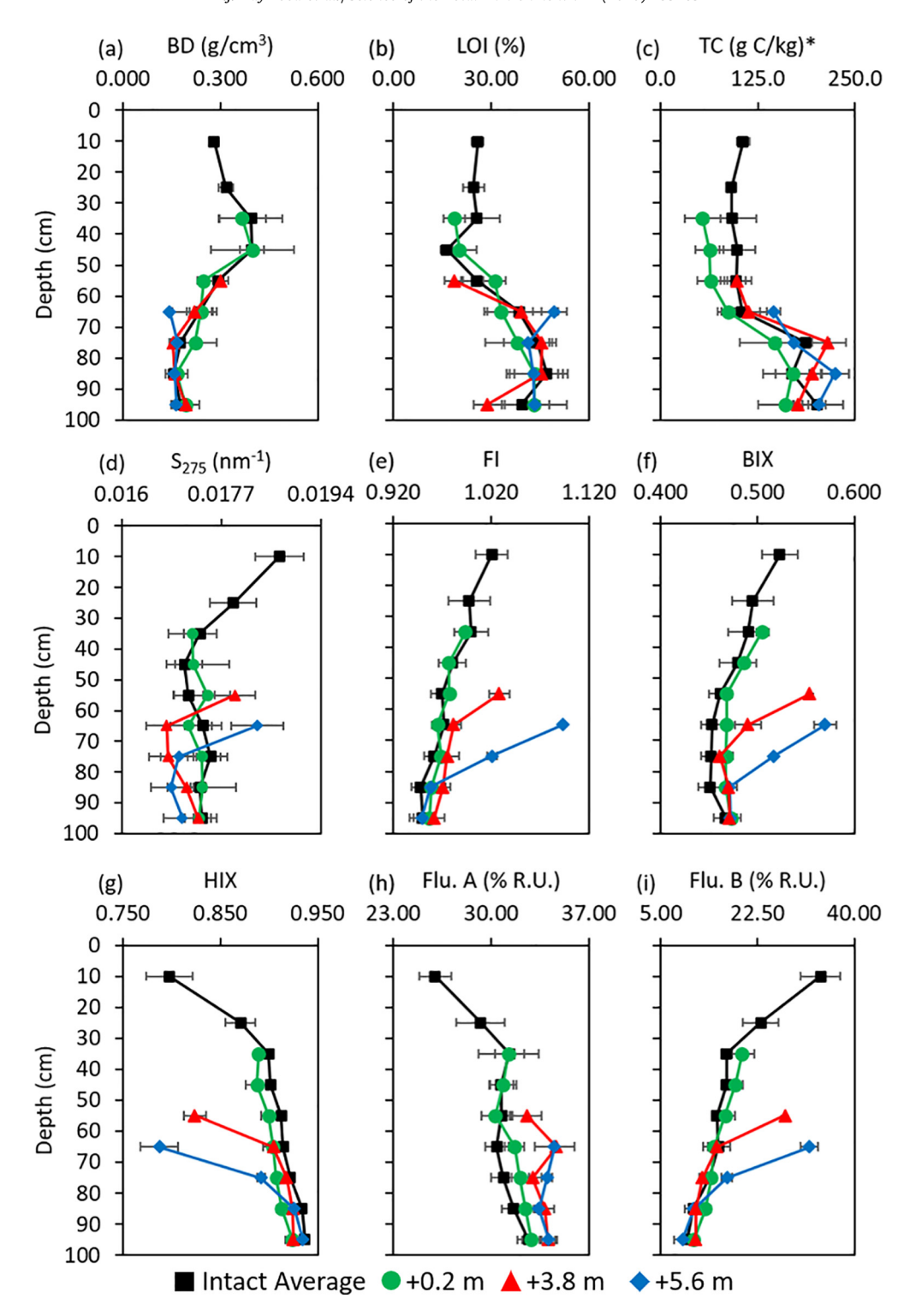


Fig. 3. Horizontally aligned mean values for geophysical and spectroscopic measurements (standard error of mean) of average intact –2.0 and –1.0 m sites (top 0–20 cm and additional 10 cm sections) and submerged + 0.2, +3.8, and + 5.6 m sites samples: (a) bulk density (BD); (b) loss on ignition (LOI); (c) total carbon (TC) (* from March 10, 2017 data); (d) spectral slope 275–295 nm (S₂₇₅); (e) fluorescence index (FI); (f) biological index (BIX); (g) humification index (HIX); (h) Fluorophore A (Flu. A); and (i) Fluorophore B (Flu. B).

the cores to the deeper layers, highlights a transition from aerobic conditions at the soil surface to anaerobic conditions at greater depths (Vaccare et al., 2019).

3.3. Horizontal trends

The identical vertical trends of the intact and submerged sites were further examined through a comparison of data by

horizontally aligning the submerged sites with the intact sites in terms of depth (Fig. 2). For the vast majority of the 30–100 cm depth samples, the mean values of BD, LOI, and TC of the submerged sites are within one standard error to those obtained for the intact sites average (Fig. 3). The submerged sites' soil is similar to that from the intact sites based on these geophysical properties. This finding indicates that the submerged sites were formed under similar environmental conditions *in situ*.

All of the spectroscopic indicators' values of the submerged site + 0.2 m, located closest to the intact marsh, are similar (within one standard error) with depth (equivalent to the intact depths of 30-100 cm) to the values for the intact sites' average (Fig. 3 (d) through (i)). The similarities of the spectroscopic indicator values suggest that the OM stored at the + 0.2 m site is characteristically similar to that of the intact sites of the same depth, see Fig. 2. Moving further away from the edge of the intact marsh, the spectroscopic indicator values for the top layers (equivalent to depth of 50-60 and 60-70 cm, respectively) of the + 3.8 m and + 5.6 m sites show increased deviations from the corresponding values obtained for the intact sites at equivalent depths (Fig. 3 (d) through (i)). Overall, this indicates that the characteristic changes of the OM present in the top layers of submerged sites + 3.8 m and + 5.6 m resulting from abiotic and biotic degradation of the OM at these locations.

Spectroscopic indicators (Fig. 3 (d) and (g) through (h)) reveal that the middle 10 cm sections of the submerged sites + 3.8 m and + 5.6 m (60-70 cm and 70-80 cm, respectively, see Fig. 2) have very similar OM to that of the intact sites at the same depths. The FI and BIX data indicate that the surface OM is undergoing more abiotic and biotic degradation at the + 5.6 m site compared to the buried equivalent soil at the + 3.8 m site (Fig. 3 (e) and (f)). The decrease in degradation continues with depth, as indicated by the nearly identical (within one standard error) spectroscopic indicator values of sites + 3.8 m and + 5.6 m at depths of 70-100 and 80-100 cm, respectively, to those of the + 0.2 m site (Fig. 3 (d) through (i)). This decrease in degradation with depth would not be observed if OM eroded from the marsh was simply reburied at the submerged sites. Instead, this trend suggests a constant degradation of newly exposed surface OM at the submerged sites that is peeled away by erosive force, exposing a fresh surface layer. The intact, fibrous nature of the peat at the submerged sites also supports this conclusion. A more in-depth examination of these horizontal trends is presented in Supporting Information S5.

3.4. Interactions at the soil-water interface

Exposure of the OM in the top (10 cm) layer of sites + 3.8 m and + 5.6 m to the oxygen-rich (oxic) bay water at the soil-water interface is hypothesized to be the cause of the deviation of the spectroscopic indicators' values from their aligned intact marsh counterparts (Fig. 3). The approximate thousand-fold, i.e., g versus mg per kg (Table S3.2) difference between the carbon content of the marsh soil and the pore water results in a concentration gradient and hence leaching of the carbon from the soil organic matter to the pore water. While the possibility of a simple mixing of the Bay's oxic water OM with the top (10 cm) layer of submerged sites OM was considered, utilizing carbon as a conservative tracer, it was determined not to be the sole cause of the observed changes in the values of the spectroscopic indicators, with leaching as well as abiotic and biotic degradation contributing significantly to these changes (see Supporting Information S6 for details). The effects of the soil-water interface on the submerged sites were examined through the comparison of mean transect top 10 cm sections (i.e., 30-40 cm; 50-60 cm; and 60-70 cm for the + 0.2 m, +3.8 m, and + 5.6 m site, respectively, see Fig. 2) indicator values (Fig. 3 and Table 2 and S3.2). An increase in dilution, leaching, abiotic and biotic degradation of the OM in submerged sites' top 10 cm sections was indicated by the decrease in DOC concentration across the transect from + 0.2 m to + 5.6 m (Table 2). A transition from refractory OM at + 0.2 m to labile OM at + 5.6 m in the top 10 cm was indicated by a decrease in MW of lignin-like compounds (inverse S₂₇₅ value) and degree of humification (HIX) across the transect (Fig. 3). Both abiotic and biotic degradation of the OM in the submerged sites' top 10 cm across the transect was indicated by the statistically significant (p < 0.05) decrease in the terrestrial nature of the OM (inverse FI value) and the increase in OM "freshness" (BIX) (Fig. 3). Increased biotic degradation across the top layer of the submerged sites along the transect is further indicated by the increase in the percent intensity of aquatic-like sourced OM (Fluorophore A) as well as the statistically significant (p < 0.05) increase in protein-like sourced OM (Fluorophore B) (Fig. 3).

Overall, the longer the OM is exposed in the top layer, at the soil–water interface, the greater its degradation. This is seen by the increase in degradation processes and overall change in spectroscopic indicator values for + 0.2 m to + 5.6 m sites, as compared to the corresponding average intact site values (Fig. 3). This results in a slow release of the carbon stored in these submerged sites through leaching, followed by degradation, and is predicted to continue layer by layer, causing the loss in OM in the 80–100 cm and 90–120 cm for + 3.8 m and + 5.6 m sites (Fig. 2), respectively. Given the larger carbon concentrations in the deeper depths of the marsh compared to the top surface \sim 0–20 cm sections, it can be concluded that oxygenation of the constantly eroding soil-water interface results in a greater liberation of carbon from the submerged sections of marsh than from the intact marsh for the top, \sim 0–20 cm, layer.

3.5. Eroding marsh fate

Previous research has shown that the marsh edge erodes due to an instability caused by small waves excavating the fine muds from below the 20 cm rhizosphere, causing intact portions of the marsh to tear off the edge and collapse into the open bay (Sapkota and White, 2019; Valentine and Mariotti, 2019). There are two possible fates of the collapsed marsh's OM at this point i) the OM either falls and becomes incorporated into the submerged sediment of the adjacent estuary, becoming reburied over time, or ii) the OM is exposed to the oxygenated bay water and is both physically transferred out into the bay and further degraded (by physical fragmentation, abiotic and biotic degradation, etc.), with the ultimate result being the loss of the stored carbon. The actual fate-burial or exposure-can be distinguished by identifying the submerged sites' dissolved OM, as degradation processes will be indicated in the aqueous phase. Therefore, specific focus is placed on the + 0.2 m (water's edge) site due to its close proximity to the eroding edge and, potentially, more recent deposition.

The + 0.2 m 30-40 cm mean values of BD, LOI, and TC are statistically significantly (p < 0.05) different from the "intact marsh model" values, represented by the average value for -2.0 m and -1.0 m 0-20 cm (Fig. 3 and Table S3.2). The following characteristics of the OM isolated from the + 0.2 m 30-40 cm were significantly higher (p < 0.05) when compared to the "intact marsh model": MW of lignin-like compounds (inverse S₂₇₅ value); degree of humification (HIX); and terrestrial nature (FI) (Fig. 3 and Table S3.2). These combined measurements indicate that the eroding edge contains more labile OM and the + 0.2 m OM is more terrestrial and refractory in nature than the "intact marsh model" soils. A shift from labile to refractory OM would not likely occur in the bay during a reburial process, which would preserve the organic matter. Instead, the eroding edge OM upon collapse and exposed to and degraded in the bay water with resulting leaching of the porewater DOC. Other researchers have previously ²¹⁰Pbdated the submerged peat deposits and have found that below 2 cm from the surface, the age of the peat exceeds the threshold for ²¹⁰Pb dating (~ 100 yrs) which supports our finding that eroded marsh peat is not being reburied within the bay in close proximity to the marsh edge (Wilson and Allison 2008). In addition, Vaccare et al. (2019) found a thin veneer of fine inorganic mud covering the intact peat at sites 40-60 m from the marsh overlying intact peats,

Table 2
Transect mean (standard error of mean) indicator values of intact marsh "intact marsh model" -2.0 m and -1.0 m (0-20 cm) (n = 12), top 10 cm sections of submerged sites + 0.2 m, +3.8 m, and + 5.6 m (n = 3), and surface water (n = 3).

Measurement	-2.0 m and -1.0 m (0-20 cm)	+0.2 m (30-40 cm)	+3.8 m (50-60 cm)	+5.6 m (60-70 cm)	Surface
DOC (mg C/L) BIX	42.893 (5.596) 0.523 (0.027)	30.204 (6.609) 0.504 (0.005)	26.183 (1.395) 0.554 (0.005)	23.775 (2.960) 0.570 (0.014)	19.628 (0.139)* 0.630 (0.012)*
Fluorophore A (% R.U.)	25.975 (1.301)	31.217 (2.152)	32.559 (1.039)	34.539 (1.411)	42.245 (0.264)*

^{*}Statistically significant (p < 0.05) difference between the surface water and pore water of the model eroding edge and submerged sites top layer.

suggesting no recent organic matter deposition, similar to the findings of Wilson and Allison (2008). This conclusion is further supported by the horizontal matching of the + 0.2 m and average intact marsh OM from 40 cm down which demonstrates significant degradation (Table S5.1).

3.6. Fate of OM in surface water

The well mixed nature of the bay's surface water makes determining its exact OM source (e.g., eroded marsh edge ~ 0-20 cm and/or leaching submerged marsh) analytically challenging. The continual input (leaching), dilution changes, and the short lifespan of the OM in the bay's surface water add to the complexity of source and transformation identification. The OM in the pore water of the intact marsh -2.0 m and -1.0 m ($\sim 0-20$ cm) and the submerged marsh + 0.2, +3.8, and + 5.6 m (top 10 cm) were compared to the surface water OM to identify any transformations (Table 2). The surface water has a statistically significant (p < 0.05) lower DOC concentration, compared to the pore water of the intact and submerged marsh, which indicates mainly dilution as well as abiotic and/or biotic degradation (Table 2). Abiotic and biotic degradation of the OM in the surface water is indicated by the statistically significant (p < 0.05) increase in the OM "freshness" (BIX) and aquatic-like sourced OM (Fluorophore A) as compared to the DOM in the intact and submerged marsh pore water (Table 2). Overall, the continual exposure of eroding OM and leaching of OM into the surface water results in abiotic and biotic degradation and loss of stored soil carbon.

3.7. Synthesis

The OM at all sites along the sampling transects was formed when the studied island was a continuous vegetated marsh and prior to the current tidal/wave erosion. During that time period, the OM was stored through the vertical accumulation of the marsh and transformed from labile OM to refractory OM, under aerobic (top layers) and anaerobic (deeper layers) conditions. This process led to increased carbon content and humification as well as decreased biotic degradation with depth that was identified at all sites across the transects, as summarized in Fig. 4 as transformation (a), with associated data presented in Table S4.1 and Fig. 3.

The physical and chemical changes caused by the tidal/wave erosion can be described as a stepwise process that begins with the erosion of the top \sim 0–20 cm of the marsh's edge and its eventual collapse into the bay. Once collapsed, this bulk section is not reburied but exposed to wave action and the aerobic condition of the bay surface water, as shown in Fig. 4; transformation (b). With the 0–20 cm section removed, the OM stored below becomes submerged and more easily eroded due to the removal of the living root matrix. Once submerged, the soil is exposed to the aerobic bay water through the soil-water interface. As the surface is inundated and eroded, the soil OM leaches out and degrades as identified by the indicator changes shown in Fig. 4 as transformation (c), with associated data presented in Fig. 3 and Table S3.2. Through this inundation and continual erosion of the soil-water interface, the OM in the submerged sites undergoes leaching, dilution,

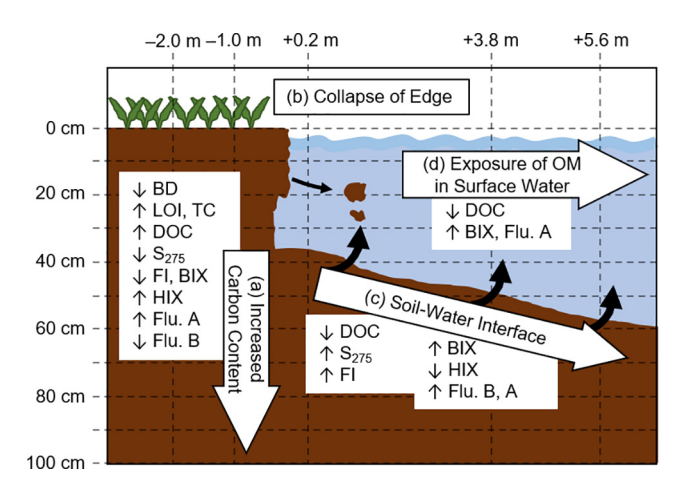


Fig. 4. Diagram of the carbon cycling over a cross-section of the study site transect. The transformation processes determined are shown by the overall change in indicator values with: (a) vertical increase in carbon content, humification of the stored carbon, and decrease in biotic degradation with depth; (b) collapse of the eroding marsh edge ~ 20 cm section OM into the bay water (thin arrow); (c) soilwater interface resulting in leaching (thick arrows), dilution, abiotic, and biotic degradation of submerged sites top layer of OM, with an increase in degree of degradation the longer the top layer is exposed (i.e., distance from edge); and (d) exposure of the OM (introduced from the eroding marsh edge and submerged marsh) in surface water resulting in dilution, abiotic, biotic degradation, and overall loss of OM.

abiotic, and biotic degradation, with increasing impact the longer the top layer is exposed (i.e., distances from edge). As this occurs, layer by layer, the carbon previously stored is lost and the process continues to the depth of the wave scour. Once exposed in the surface water, the OM, introduced from the eroded marsh edge and the submerged marsh, undergoes further dilution, abiotic, and biotic degradation, as shown by the indicators presented in Fig. 4 as transformation (d) and the associated data presented in Table 2.

Since 2011, the study site in Barataria Bay has experienced 847 m² of land loss, as determined by time lapse analysis of Google Earth images (Fig. 1). Using this area and the depth profile across the estuary, a total of 423.5 m³ of the marsh were eroded. Based on the BD, LOI, and TC values for 0–70 cm sections of the -2.0~mand -1.0 m sites, that equals a total of 6.56 ± 0.943 MT of OM lost per year or 2.636 \pm 0.449 MT C yr⁻¹. Based on these values and assuming similar carbon losses across the Barataria Bay (Sapkota and White, 2019, Wilson and Allison, 2008) one can conservatively estimate $\sim 1.00 \times 10^6$ metric tons of stored carbon are released annually from Barataria Bay, assuming the OM at the study site is equivalent to the other eroding wetlands of Barataria Bay, and at the current predicted coastal land loss rate of $\sim 25.9 \text{ km}^2 \text{ v}^{-1}$. This amount of carbon is the equivalent to over approximately half a million kg of coal burned each year. Globally, this large pool of soil carbon is a significant potential input of CO2 to the atmospheric CO₂ pool, especially when considering coastal wetlands under threat of rising sea level. This carbon pool can potentially erase or overwhelm any CO2 reduction strategies realized by humans going forward, underscoring the need for coastal wetland preservation/restoration strategies (Sapkota and White, 2020).

4. Conclusions

This study found that substantial carbon loss is associated with erosion of coastal wetlands in Barataria Bay, LA, and is concomitant with a relative sea level predicted for the world's stable coastlines in 50–75 years. Geophysical and spectroscopic analyses find that the eroded wetland soil carbon is not reburied in the adjacent estuary, but that submerged carbon continues to be eroded and degraded until the estuary reaches a steady state depth of $\sim 1.5~\text{m}$. This wetland soil carbon pool is a potential significant contributor to the atmospheric CO2 pool and underscores the need for present day and future preservation of coastal wetland soil carbon stocks to prevent overwhelming humanity's efforts in slowing or reducing CO2 concentrations in the atmosphere.

Declaration of Competing Interest

The authors declare that they have no known competing financial interests or personal relationships that could have appeared to influence the work reported in this paper.

Acknowledgement

This work was supported by the National Science Foundation under grants CHE-1411547 and OCE-1636052. Special thanks to Eddie Weeks who's logistical and sampling expertise made this research possible and thanks to Quintin Picard and Amanda Fontenot for their help with sample collecting and processing.

Appendix A. Supplementary data

Supplementary data to this article can be found online at https://doi.org/10.1016/j.scitotenv.2019.135185.

References

- Bianchi, T.S., Cook, R.L., Perdue, E.M., Kolic, P.E., Green, N., Zhang, Y., Smith, R.W.,
 Kolker, A.S., Ameen, A., King, G., 2011. Impacts of diverted freshwater on dissolved organic matter and microbial communities in Barataria Bay,
 Louisiana, USA. Mar. Environ. Res. 72 (5), 248–257.
 Chmura, G.L., Anisfeld, S.C., Cahoon, D.R., Lynch, J.C., 2003. Global carbon
- Chmura, G.L., Anisfeld, S.C., Cahoon, D.R., Lynch, J.C., 2003. Global carbon sequestration in tidal, saline wetland soils. Global Biogeochem. Cycles 17 (4). Choi, Y., Wang, Y., 2004. Dynamics of carbon sequestration in a coastal wetland
- using radiocarbon measurements. Global Biogeochem. Cycles 18 (4).
- Chow, A.T., Dai, J., Conner, W.H., Hitchcock, D.R., Wang, J., 2012. Dissolved organic matter and nutrient dynamics of a coastal freshwater forested wetland in Winyah Bay, South Carolina. Biogeochemistry 112 (1–3), 571–587.
- Clark, C., Aiona, P., Keller, J., Bruyn, W.D., 2014. Optical characterization and distribution of chromophoric dissolved organic matter (CDOM) in soil porewater from a salt marsh ecosystem. Mar. Ecol. Prog. Ser. 2014 (516), 71–83.
- Cook, R.L., Birdwell, J.E., Lattao, C., Lowry, M., 2009. A multi-method comparison of Atchafalaya Basin surface water organic matter samples. J. Environ. Qual. 38 (2), 702–711.
- DeLaune, R.D., Nyman, J.A., Patrick Jr, W., 1994. Peat collapse, ponding and wetland loss in a rapidly submerging coastal marsh. J. Coastal Res., 1021–1030
- Fichot, C.G., Benner, R., 2012. The spectral slope coefficient of chromophoric dissolved organic matter (\$275-295\$) as a tracer of terrigenous dissolved organic carbon in river-influenced ocean margins. Limnol. Oceanogr. 57 (5), 1453-1466.
- FitzGerald, D.M., Fenster, M.S., Argow, B.A., Buynevich, I.V., 2008. Coastal impacts due to sea-level rise. Annu. Rev. Earth Planet. Sci. 36, 601–647.
- Haywood, B.J., White, J.R., Cook, R.L., 2018. Investigation of an early season river flood pulse: Carbon cycling in a subtropical estuary. Sci. Total Environ. 635, 867–877.
- Hoogsteen, M., Lantinga, E., Bakker, E., Groot, J., Tittonell, P., 2015. Estimating soil organic carbon through loss on ignition: effects of ignition conditions and structural water loss. Eur. J. Soil Sci. 66 (2), 320–328.
- Huguet, A., Vacher, L., Relexans, S., Saubusse, S., Froidefond, J.-M., Parlanti, E., 2009. Properties of fluorescent dissolved organic matter in the Gironde Estuary. Org Geochem. 40 (6), 706–719.

- Kolic, P.E., Roy, E.D., White, J.R., Cook, R.L., 2014. Spectroscopic measurements of estuarine dissolved organic matter dynamics during a large-scale Mississippi River flood diversion. Sci. Total Environ. 485, 518–527.
- Kolker, A.S., Allison, M.A., Hameed, S., 2011. An evaluation of subsidence rates and sea-level variability in the northern Gulf of Mexico. Geophys. Res. Lett. 38 (21).
- Kothawala, D.N., Murphy, K.R., Stedmon, C.A., Weyhenmeyer, G.A., Tranvik, L.J., 2013. Inner filter correction of dissolved organic matter fluorescence. Limnol. Oceanogr. Methods 11 (12), 616–630.
- Levine, B., White, J., DeLaune, R., Maiti, K., 2017. Crude oil effects on redox status of salt marsh soil in Louisiana. Soil Sci. Soc. Am. J. 81 (3), 647–653.
- Li, C., White, J.R., Chen, C., Lin, H., Weeks, E., Galvan, K., Bargu, S., 2011. Summertime tidal flushing of Barataria Bay: transports of water and suspended sediments. J. Geophys. Res. 116.
- Matear, R.J., 2004. Ocean Carbon cycle in a changing climate: climate change detection. The Ocean Carbon Cycle and Climate, 297–315.
- McKnight, D.M., Boyer, E.W., Westerhoff, P.K., Doran, P.T., Kulbe, T., Andersen, D.T., 2001. Spectrofluorometric characterization of dissolved organic matter for indication of precursor organic material and aromaticity. Limnol. Oceanogr. 46 (1), 38–48.
- Mcleod, E., Chmura, G.L., Bouillon, S., Salm, R., Björk, M., Duarte, C.M., Lovelock, C.E., Schlesinger, W.H., Silliman, B.R., 2011. A blueprint for blue carbon: toward an improved understanding of the role of vegetated coastal habitats in sequestering CO₂. Front. Ecol. Environ. 9 (10), 552–560.
- Ohno, T., 2002. Fluorescence inner-filtering correction for determining the humification index of dissolved organic matter. Environ. Sci. Technol. 36 (4), 742–746.
- Parlanti, E., Wörz, K., Geoffroy, L., Lamotte, M., 2000. Dissolved organic matter fluorescence spectroscopy as a tool to estimate biological activity in a coastal zone submitted to anthropogenic inputs. Org Geochem. 31 (12), 1765–1781.
- Penland, S., Wayne, L., Britsch, L., Williams, S.J., Beall, A.D., Butterworth, V.C., 2000. Process classification of coastal land loss between 1932 and 1990 in the Mississippi River delta plain, southeastern Louisiana; 2331–1258.
- Perie, C., Ouimet, R., 2008. Organic carbon, organic matter and bulk density relationships in boreal forest soils. Can. J. Soil Sci. 88 (3), 315–325.
- Pfeffer, W.T., Harper, J., O'Neel, S., 2008. Kinematic constraints on glacier contributions to 21st-century sea-level rise. Science 321 (5894), 1340–1343.
- Reddy, K.R., DeLaune, R.D., 2008. Biogeochemistry of wetlands: science and applications. CRC Press.
- Sapkota, Y., White, J.R., 2019. Marsh edge erosion and associated carbon dynamics in coastal Louisiana: a proxy for future wetland-dominated coastlines worldwide. Estuar. Coast. Shelf Sci. 226, 106–289.
- Sapkota, Y., White, J.R., 2020. Carbon offset market methodologies applicable for coastal wetland restoration and conservation in the United States: a review. Sci. Total Environ. 701, 134497.
- Spencer, T., Schuerch, M., Nicholls, R.J., Hinkel, J., Lincke, D., Vafeidis, A., Brown, S., 2016. Global coastal wetland change under sea-level rise and related stresses: The DIVA wetland change model. Global Planet. Change 139, 15–30.
- USGS (United States Geological Survey), 2017. National Water Informatino Systyem. https://waterdata.usgs.gov/usa/nwis/uv?07380251 (accessed November, 2017).
- Steinmuller, H.E., Dittmer, K.M., White, J.R., Chambers, L.G., 2019. Understanding the fate of soil organic matter in submerging coastal wetland soils: a microcosm approach. Geoderma 337, 1267–1277.
- Vaccare, J., Meselhe, E., White, R.J., 2019. The denitrification potential of eroding wetlands in Barataria Bay, LA, USA: implications for river reconnection. Sci. Total Environ. 686, 529–537.
- Valentine, K., Mariotti, G., 2019. Wind-driven water level fluctuation drive marsh edge erosion variability in microtidal coast bays. Cont. Shelf Res. 2019 (176), 76–89.
- Van de Broek, M., Temmerman, S., Merckx, R., Govers, G., 2016. Controls on soil organic carbon stocks in tidal marshes along an estuarine salinity gradient. Biogeosciences 13 (24), 6611.
- Vermeer, M., Rahmstorf, S., 2009. Global sea level linked to global temperature. Proc. Natl. Acad. Sci. 106 (51), 21527–21532.
- Wang, Y., Zhang, D., Shen, Z., Feng, C., Chen, J., 2013. Revealing sources and distribution changes of dissolved organic matter (DOM) in pore water of sediment from the Yangtze estuary. PLoS ONE 8, (10) e76633.
- Watanabe, A., McPhail, D.B., Maie, N., Kawasaki, S., Anderson, H.A., Cheshire, M.V., 2005. Electron spin resonance characteristics of humic acids from a wide range of soil types. Org Geochem. 36 (7), 981–990.
- Weishaar, J.L., Aiken, G.R., Bergamaschi, B.A., Fram, M.S., Fujii, R., Mopper, K., 2003. Evaluation of specific ultraviolet absorbance as an indicator of the chemical composition and reactivity of dissolved organic carbon. Environ. Sci. Technol. 37 (20), 4702–4708.
- Wilson, Carol A., Allison, Mead A., 2008. An equilibrium profile model for retreating marsh shorelines in Southeast Louisiana. Estuar. Coast. Shelf Sci. 80 (4), 483–494.
- Wright, A.L., Wang, Y., Reddy, K.R., 2008. Loss-on-ignition method to assess soil organic carbon in calcareous everglades wetlands. Commun. Soil Sci. Plant Anal. 39 (19–20), 3074–3083.